Sensible heat measurements indicating depth and magnitude of subsurface soil water evaporation

J. L. Heitman,[1] X. Xiao,[2] R. Horton,[2] and T. J. Sauer[3]

Received 29 February 2008; revised 29 June 2008; accepted 30 July 2008; published 18 October 2008.

[1] Most measurement approaches for determining evaporation assume that the latent heat flux originates from the soil surface. Here, a new method is described for determining in situ soil water evaporation dynamics from fine-scale measurements of soil temperature and thermal properties with heat pulse sensors. A sensible heat balance is computed using soil heat flux density at two depths and change in sensible heat storage in between; the sensible heat balance residual is attributed to latent heat from evaporation of soil water. Comparisons between near-surface soil heat flux density and Bowen ratio energy balance measurements suggest that evaporation originates below the soil surface several days after rainfall. The sensible heat balance accounts for this evaporation dynamic in millimeter-scale depth increments within the soil. Comparisons of sensible heat balance daily evaporation estimates to Bowen ratio and mass balance estimates indicate strong agreement (r^2 = 0.96, root-mean-square error = 0.20 mm). Potential applications of this technique include location of the depth and magnitude of subsurface evaporation fluxes and estimation of stage 2–3 daily evaporation without requirements for large fetch. These applications represent new contributions to vadose zone hydrology.

Citation: Heitman, J. L., X. Xiao, R. Horton, and T. J. Sauer (2008), Sensible heat measurements indicating depth and magnitude of subsurface soil water evaporation, *Water Resour. Res.*, *44*, W00D05, doi:10.1029/2008WR006961.

1. Introduction

[2] Soil-water evaporation is a critical component of both the surface energy balance and the hydrologic cycle, coupling heat and water transfer between land and atmosphere [*Berge*, 1990]. In drying technology [e.g., *Segura and Toledo*, 2005; *Prat*, 2007], it is widely recognized that control and location of drying (i.e., evaporation) depends on the balance between heat, liquid, and vapor transport mechanisms. Shifts between atmospheric and soil control on evaporation have been commonly referred to in the soil science and hydrology literature as stages of evaporation [*Lemon*, 1956]. The inability to quantify near-surface soil processes has prevented a detailed, accurate assessment of near-surface soil water evaporation [*Kondo et al.*, 1990; *Yamanaka and Yonetani*, 1999]. Because the balance of heat, liquid, and vapor mechanisms in soil is difficult to predict, measurement-based approaches are needed to determine dynamic behavior, particularly in the field [e.g., *Cahill and Parlange*, 1998]. *Heitman et al.* [2008] introduced a measurement-based soil sensible heat balance to determine the partitioning of latent heat within the soil, and thereby account for soil-water evaporation in situ. Such an approach offers broad potential utility because it does not require determination of coupled heat and water transfer coefficients [e.g., *Nassar and Horton*, 1997], characterization of soil-specific hydraulic properties [e.g., *Mahrt and Pan*, 1984; *Wetzel and Chang*, 1987], or large fetch. Here we present a conceptual background for the soil sensible heat balance method and provide preliminary tests using comparison to both above-ground (Bowen ratio) and mass balance (microlysimeter) estimates of evaporation.

2. Method

2.1. Conceptual Background

[3] The surface energy balance is commonly treated as

$$R_n - G = LE + H \tag{1}$$

where R_n (W m^{-2}) is net radiation, G (W m^{-2}) is surface soil heat flux density, and LE (W m^{-2}) and H (W m^{-2}) are latent and sensible heat flux densities, respectively [cf. *Cellier et al.*, 1996]. Widely used calorimetric and combination approaches for determining G rely on measurement of heat flux density below the surface. A correction is then made for change in sensible heat storage, ΔS (W m^{-2}), between the depth of measurement and the surface [*Fuchs*, 1986]:

$$G = G_o + \Delta S \tag{2}$$

where G_o refers to heat flux density measured at some arbitrary subsurface depth.

[4] Equation (2) assumes that LE originates at the soil surface rather than within the soil [*Mayocchi and Bristow*, 1995]. This is a restrictive assumption, because as soil dries from the surface downward, an increasing fraction of soil water evaporation occurs below the surface [*Yamanaka et al.*, 1998]. Micrometeorological methods (e.g., Bowen ratio

[1]Department of Soil Science, North Carolina State University, Raleigh, North Carolina, USA.
[2]Department of Agronomy, Iowa State University, Ames, Iowa, USA.
[3]National Soil Tilth Laboratory, Agricultural Research Service, United States Department of Agriculture, Ames, Iowa, USA.

0043-1397/08/2008WR006961$09.00

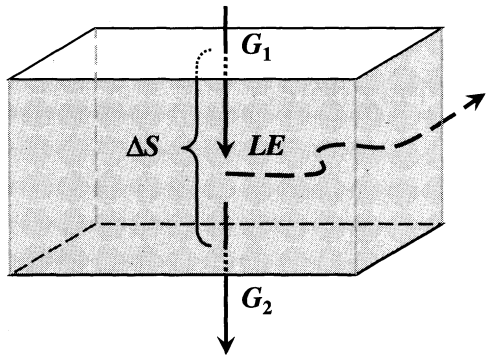

Figure 1. Conceptual model of the heat balance for a soil layer (see equation (3)). G_1 and G_2 are sensible heat flux densities at two depths; ΔS and LE are the change in sensible heat storage and the latent heat flux, respectively.

and eddy covariance) account for LE exclusively at the soil surface, but *Gardner and Hanks* [1966] suggested that (2) could be adjusted to include LE (i.e., evaporation of soil water) in order to determine evaporation occurring within the soil:

$$(G_1 - G_2) - \Delta S = LE \tag{3}$$

where G_1 and G_2 are heat flux densities measured at two different depths and ΔS represents the change in sensible heat storage between these depths (Figure 1). The hypothesis in this approach is that the residual to the balance of measurable sensible heat terms (G_1, G_2, and ΔS) represents heat partitioned to latent heat with water vaporization in the depth interval between G_1 and G_2.

[5] Instrumentation provided a major limitation for *Gardner and Hanks* [1966] and allowed mostly qualitative assessment. However, development of the heat pulse (HP) sensor [*Campbell et al.*, 1991; *Bristow et al.*, 1994; *Ham and Benson*, 2004] provides new opportunity to implement the heat balance approach. HP sensors generally consist of two or three small (1.3 mm diam) needles. One needle contains a resistance heater for applying a small heat input, while the remaining needles contain thermocouples for measuring temperature response at a fixed distance (typically 6 mm) from the heater. The temperature response can be evaluated to determine soil thermal properties. The temperature sensing needles of the sensor can also be used to passively determine ambient temperature conditions within the soil. *Cobos and Baker* [2003] and *Ochsner et al.* [2006] discussed the use of HP sensors to measure G_o, and *Ochsner et al.* [2007] discussed HP sensor measurement of ΔS. An advantage to this type of sensor is that it is relatively unobtrusive when compared to more commonly used heat flux plates. It does not appreciably limit water vapor or liquid movement and, thus, can be installed nearer the soil surface.

[6] *Heitman et al.* [2008] expanded on the approaches of *Ochsner et al.* [2006, 2007] and *Cobos and Baker* [2003] to implement (3) by measuring heat flux density at two depths (i.e., G_1 and G_2) and ΔS with a single three-needle HP sensor. In their approach, sensors, oriented perpendicular to the soil surface, are used for three functions (Figure 2): measurement of ambient temperature (T, °C), volumetric heat capacity (C, J m^{-3} °C^{-1}), and thermal conductivity (λ, W m^{-1} °C^{-1}). Examples of these data (collected as described in section 2.2) are presented in Figures 3a and 3b. The vertical T gradient, dT/dz (°C m^{-1}), is obtained by dividing the T difference by the distance, z (m), between adjacent needles (Figure 3c). The gradient can then be multiplied by λ to approximate the heat flux densities (G_1 and G_2) at the midpoint depths between adjacent needles (i.e., Fourier's law) (Figure 3d). The change in T with time, t(s), at the central needle is combined with C to determine ΔS according to *Ochsner et al.* [2007]

$$\Delta S = \sum_{i=1}^{N} C_{i,j-1} \frac{T_{i,j} - T_{i,j-1}}{t_j - t_{j-1}} (z_i - z_{i-1}) \tag{4}$$

where the subscripts i and j are index variables for depth layers and time steps, respectively (Figure 3d). For these calculations, we assume a mean thermal property (i.e., C and λ) for each sensor depth increment. Having measurements of G_1, G_2, and ΔS allows implementation of (3) to determine LE.

2.2. Measurements and Field Locations

[7] Measurements were collected at two research sites located near Ames, Iowa (41°N, 93°W), the Been field and the Brooks field. HP instrumentation at the Been field was installed in May 2007 and operated for 40 days. A bare surface area (~15,625 m^2) was maintained throughout the study. The soil at the site is Canisteo clay loam (fine-loamy, mixed, superactive, calcareous, mesic Typic Endoaquolls). In addition to HP sensors (described below), a Bowen ratio energy balance (BREB) measurement station was located 30 m from the HP instrumentation. The design of this

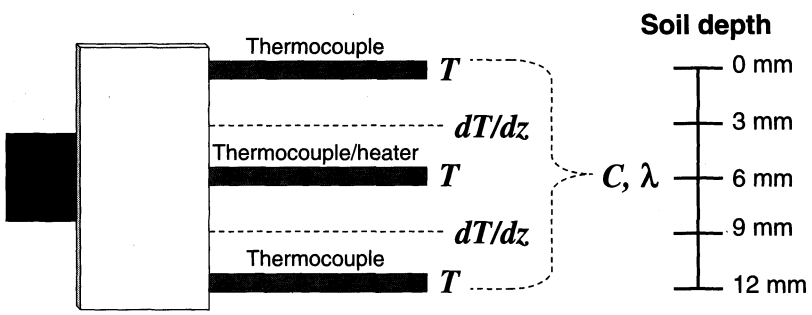

Figure 2. Heat pulse sensor measurements for implementing equation (3). Temperature, temperature gradient, volumetric heat capacity, and thermal conductivity are represented as T, dT/dz, C, and λ, respectively. The sensor is not drawn to scale.

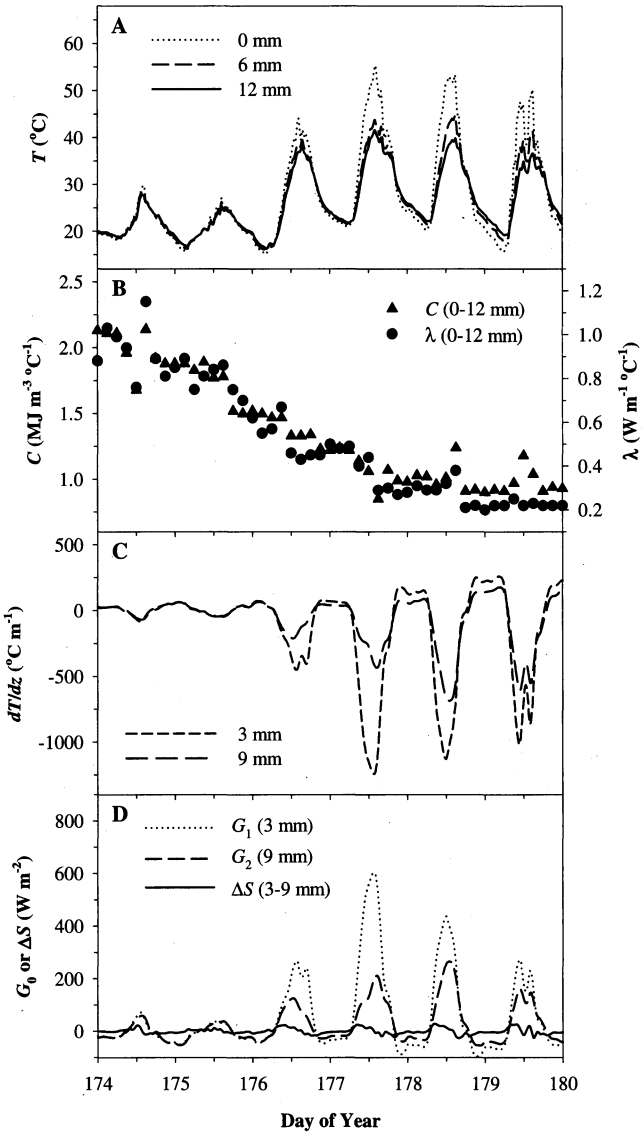

Figure 3. Measurements obtained with a heat pulse sensor for computing equation (3): (a) soil temperature (T), (b) volumetric heat capacity (C) and thermal conductivity (λ), (c) temperature gradient (dT/dz), and (d) heat flux densities (G_1 and G_2) and change in sensible heat storage (ΔS). Data were collected from the Been field following rainfall on day of year 172.

measurement system was similar to those of *Bland et al.* [1996] and *Sauer et al.* [2002]. An air temperature/relative humidity probe (model HMP45C, Vaisala Inc., Woburn, Massachusetts) was used to measure vapor pressure while a thermistor circuit was used to measure air temperature. Both sensors were mounted in aspirated radiation shields with a vertical separation of 1 m and were exchanged every 5 min. A second tripod was used to support a net radiometer (model Q*7, Radiation and Energy Balance Systems, Seattle, Washington) at a height of 2 m. Soil heat flux was measured with two flux plates (model HFT3.1, Radiation and Energy Balance Systems) at a depth of 0.06 m. Soil temperature measured with type T thermocouples at 0.015 and 0.045 m depths adjacent to each plate were used with measured volumetric water content to determine energy storage change above the flux plates [*Sauer and Horton*, 2005]. All sensor signals were monitored at a 5 s interval and 5 min averages were stored for analysis. The combined suite of instruments on the BREB station provided estimates of R_n, LE, H, and G. Fetch for the BREB station was approximately 66:1, 60:1, 16:1, and 22:1 in the south, west, north, and east directions, respectively, which is considered adequate for typical applications [*Heilman et al.*, 1989]. A tipping bucket rain gage was used to record rainfall.

[8] Experiments at the Brooks field were conducted for a 40 day measurement period beginning in late July 2005. Soil at the site is Canisteo silty clay loam. A 100 m^2 area selected for study was cleared of all vegetation and surface residue, and leveled. Estimates of soil water evaporation were obtained periodically with microlysimeters (MLs) [*Evett et al.*, 1995]. The MLs were constructed from 7.5 cm ID, white polyvinyl chloride pipe, cut to 10 cm length and milled to a wall thickness of 3 mm. The MLs were installed with a drop hammer in the area surrounding the instrument nest and not used until several natural wetting/drying cycles had occurred postinstallation. For measurements, the MLs were carefully excavated, sealed at the lower end with thin plastic, weighed in the field with a portable balance, and replaced in the soil. Evaporation estimates were determined from the change in mass upon reweighing at 24 h. At least eight replicate MLs were collected and averaged for each measurement.

[9] HP sensors built following the design of *Ren et al.* [2003] were used at both field sites. The sensors consisted of three stainless steel needles (1.3 mm diam, 4 cm length) fixed approximately 6 mm apart with an epoxy body at one end. Each needle contained a Type E thermocouple for measuring temperature; the central needle also contained a resistance heater for implementing the HP method. The sensors were calibrated in agar stabilized water to determine the apparent distance between the needles [*Campbell et al.*, 1991]. The sensors were installed via a 10 cm deep trench by pushing the needles from the trench into undisturbed soil. The plane formed by the three needles of each sensor was oriented perpendicular to the soil surface (Figure 2). Sensors were installed at six depths beginning immediately below the soil surface with the central needles of the sensors positioned at 6, 12, 18, 24, 45, and 60 mm. After installation, the sensor lead wires were routed through the trench and the trench was carefully backfilled. The sensors were connected to a data acquisition system on the soil surface, which consisted of a data logger and multiplexers for the thermocouples and heaters, all housed in a weatherproof enclosure. Power was supplied by a 12 V battery maintained with a solar panel. All heaters were controlled and measured with a single control circuit consisting of a relay and 1-Ω precision resistor. Thermal property measurements were collected each 3 h. Thermal diffusivity and C were determined following the procedures described by *Bristow et al.* [1994] and *Knight and Kluitenberg* [2004], respectively. Measurements were corrected for ambient T drift using the T measurements collected prior to HP initiation. A time-scaled change in ambient T was subtracted from the T change observed following application of the heat pulse [*Jury and Bellantuoni*, 1976; *Ochsner et al.*, 2006]. Soil thermal conductivity λ was computed as the product of the thermal diffusivity and C. Thermocouples in each sensor needle were used to record

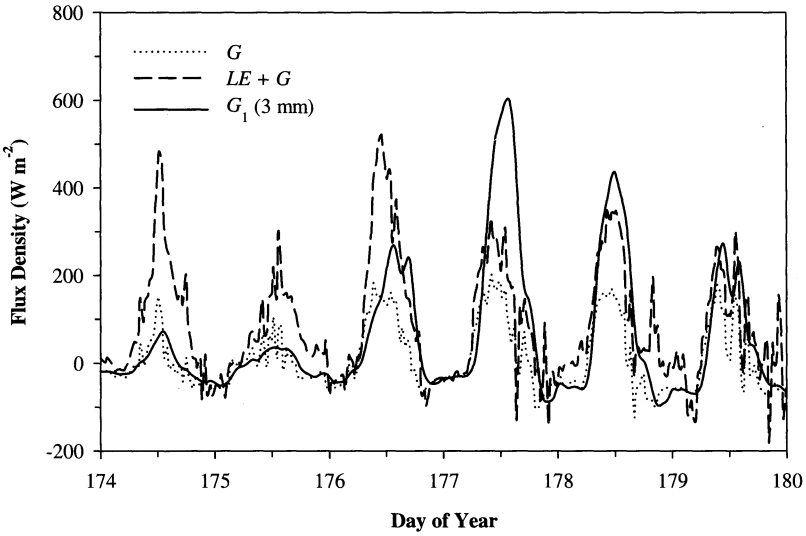

Figure 4. Comparison of heat pulse measured heat flux density for the 3 mm soil depth (G_1) and independent measurements of latent heat flux density (LE) and surface soil heat flux (G) obtained with the Bowen ratio energy balance measurement station at the Been field.

ambient soil T each 30 min (5 min average). Measurements of T, C, and λ were used together as described above to determine LE for a discrete depth increment with each sensor. *Heitman et al.* [2008] provides additional details on data handling.

3. Results and Discussion

3.1. Evidence of Evaporation Below the Soil Surface

[10] The general hypothesis in the sensible heat balance approach is that evaporation occurs below the soil surface, and therefore, can be determined by measurements within the soil. A limitation in testing this hypothesis is the proximity to the surface in which the uppermost heat flux G_1 can be measured. The practical limit for G_1 with the design of the heat pulse sensors used in these experiments is approximately 3 mm, which is the midpoint between needles installed immediately at the surface and the adjacent needle positioned at 6 mm below the surface (Figure 2). This prevents measurement of evaporation occurring above the 3 mm soil depth where it likely occurs in the day(s) immediately following rainfall or irrigation. However, if the evaporation front does penetrate deeper into the soil, it should be discernable. To test this idea we compare heat flux density measured at the 3 mm soil depth in the Been field with measurements obtained from the BREB measurement station (Figure 4).

[11] Data in Figure 4 were collected following a rainfall event on day of year (DOY) 172. If evaporation occurs below 3 mm in the soil, then G_1 at the 3 mm depth should be approximately equal to the sum of LE and G as treated in (1) and measured by the BREB station. It is clear that $LE + G$ exceeds G_1 until DOY 176, suggesting that evaporation is occurring above the 3 mm soil depth. However, on DOY 176 G_1 increases and begins to exceed G. The growing peak magnitude of G_1, while still remaining less than $LE + G$, suggests that some but not all evaporation is occurring below the 3 mm depth. DOY 177 provides an anomaly where G_1 actually exceeds $LE + G$. This result is surprising and suggests error in either the BREB station or G_1. While the magnitude of the 3 mm heat flux density is exceptionally large and cannot be confirmed independently, we note that the magnitude of DOY 177 $LE + G$ also differs from the general trend on DOY 176–181. Despite similar conditions on the days before and after, H measured with the BREB on DOY 177 was uncharacteristically large and suggests some measurement error (data not shown). DOY 177 represents a transition to evaporation below the 3 mm depth in the soil. On subsequent days, G_1 decreases and begins to track closely with the magnitude of $LE + G$. The pattern revealed by this comparison indicates that the measurements of near-surface heat flux density accurately depict $LE + G$ following stage 1 evaporation.

3.2. Subsurface Evaporation Patterns

[12] The comparison between $LE + G$ and G_1 suggests that some evaporation is occurring below the 3 mm depth beginning on DOY 176. To quantify this evaporation we utilize measurements for multiple depth increments below the soil surface, where each depth increment includes G_1, G_2, and ΔS measured by a single sensor. These data are shown for the uppermost sensor in Figure 3. During this time period, daily maximum ambient T generally increases after rainfall through DOY 178 at the 0, 6, and 12 mm depths (Figure 3a). Drying in the upper portion of the soil profile also produces declines in both C and λ (Figure 3b). Accompanying these changes are shifts in the magnitude of dT/dz at the 3 and 9 mm depths. The magnitude of dT/dz is similar with depth through DOY 175 (Figure 3c). On DOY 176, the peak magnitude of dT/dz at 3 mm begins to increase and thereafter remains relatively large. A shift also occurs at 9 mm on DOY 176, but peak magnitudes remain well below those at 3 mm until DOY 178 when the gradients begin to converge. This indicates that drying occurs deeper in the soil. Driven by dT/dz, heat flux density demonstrates a similar pattern (Figure 3d). The 3 and 9 mm depth heat flux densities are nearly identical through DOY 175. However, beginning on DOY 176, divergence in the heat flux density with depth indicates significant heat loss

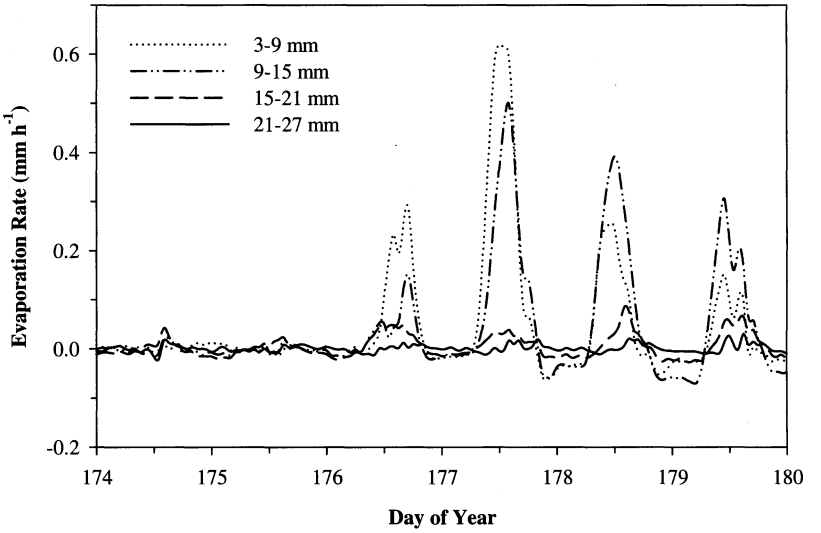

Figure 5. Evaporation determined by heat balance (equation (3)) using heat pulse sensors. Data were collected from the Been field following rainfall on day of year 172.

(>150 W m^{-2}) as heat is transferred through the soil. The amount of heat partitioned to ΔS can be quantified and remains consistently small throughout this period (<25 W m^{-2}). The difference between heat flux density at 3 and 9 mm (i.e., G_1 and G_2) appreciably exceeds ΔS through DOY 178 and thereby provides means for determining LE with (3).

[13] Results for sensors measuring the 3–9, 9–15, 15–21, and 21–27 mm depth increments are shown in Figure 5. Note that data are presented as evaporation rate, E (mm h^{-1}), rather than LE. To make this conversion we estimate L as a function of T following *Horton* [1989]. The evaporation rate remains near zero for all measured depth increments through DOY 175, which again indicates that the evaporation zone has not passed below the 3 mm soil depth. All sensible heat transferred through the 3 mm depth is accounted for through ΔS or heat flux density at lower depths. On DOY 176, the peak magnitude of E increases to 0.3 and 0.15 mm h^{-1} during the afternoon at the 3–9 and 9–15 mm depth increments, respectively. The peak magnitude of E continues to increase for both depth increments on DOY 177 before declining on subsequent days. Despite some concerns raised above about observations on DOY 177, the pattern here again suggests a transition. Net evaporation rates are generally highest immediately following rainfall, assuming that atmospheric demand is not limiting [*Lemon*, 1956]. Thus, the relatively lower E on DOY 176 than 177 does not necessarily suggest less total evaporation. Rather it indicates that evaporation is still occurring in the soil layer above the 3 mm depth on DOY 176. Transition to evaporation at deeper soil depths is beginning to occur on DOY 176 as soil water stored above the 3 mm depth is depleted and cannot meet atmospheric demand. After DOY 177, measurements of the 3 mm heat flux density (Figure 4) suggest that nearly all evaporation occurs below the 3 mm soil depth. The shifting pattern of evaporation continues on subsequent days as soil water storage is further depleted near the surface and peak E at 9–15 mm begins to exceed E at 3–9 mm (Figure 5). The declining peak magnitudes of E for all depth increments after DOY 177 are indicative of decreased total evaporation as soil water becomes limiting.

3.3. Comparison of Heat Balance Daily Evaporation to Independent Estimates

[14] An advantage of the heat balance approach is that it allows observation of in situ evaporation for multiple depth increments below the soil surface, whereas other methods such as Bowen ratio and lysimeters only provide indication of total net evaporation. Yet this also provides some difficulty for verifying the data presented in Figure 5. Few means are available for temporal comparison to fine-scale soil water evaporation measurements. In order to provide a means for comparison, we take a daily sum of the values from (3) for all measured depth increments to obtain an estimate of total daily evaporation. These estimates are compared to total daily evaporation determined by microlysimeters at the Brooks field and the Bowen ratio approach at the Been field in Figure 6. We assume a priori that measurements from the heat pulse sensors do not capture evaporation occurring above the 3 mm soil depth immediately after rainfall as discussed above. Thus, comparisons in Figure 6 preclude measurements taken in the first 3 days after rainfall.

[15] Daily evaporation estimates from the independent estimates (microlysimeter and Bowen ratio) ranged from 3.29 to 0.57 mm (Figure 6). Regression analysis indicates strong correlation between the heat balance and independent estimates with r^2 = 0.96 and root-mean-square error (RMSE) = 0.20 mm for 20 days of measurements. The regression relationship is also near 1:1 with slope of 0.91 and intercept of 0.16. Treated independently, the relationship between heat balance and microlysimeter estimates (available on 9 days) gave slightly lower RMSE (0.11 mm). The range of the compared observations from the microlysimeters was limited to <1.5 mm daily evaporation by environmental conditions during the Brooks field experiment. However, the reduced error may indicate the improved accuracy of the method under predominantly

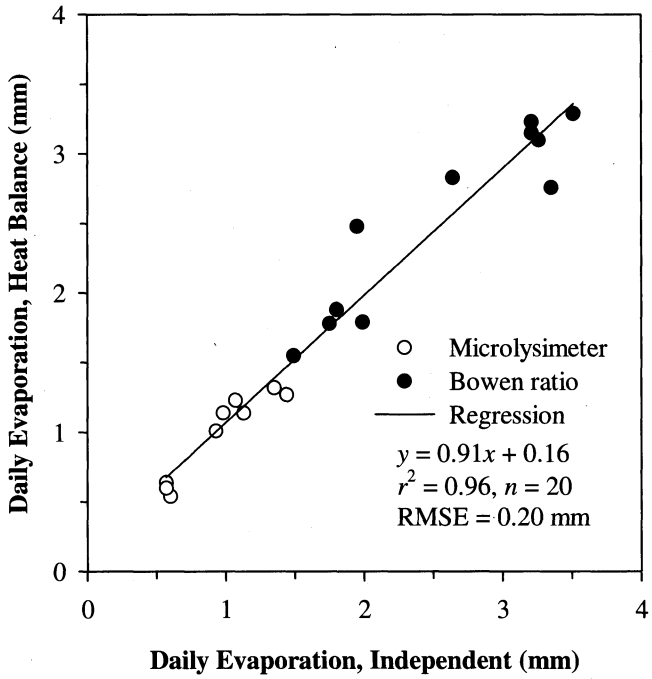

Figure 6. Comparison of daily evaporation obtained by the heat balance and two independent methods (Bowen ratio and microlysimeters). Data included in Figure 6 were obtained 3 days or more after rainfall events. Data from DOY 177 at the Been field have been omitted.

water-limited (i.e., soil-controlled) evaporative conditions. Overall, comparisons between heat balance and independent estimates of total daily evaporation indicate the potential of the heat balance method. Though indirect, these comparisons also provide support for the fine time and depth scale measurements of evaporation from which the heat balance daily estimates were derived.

4. Summary and Conclusions

[16] Few if any measurement approaches are currently available for determining in situ soil water evaporation. However, developments in the HP measurement technique provide a new opportunity to implement such an approach. Here, measurements of soil temperature and thermal properties obtained with HP sensors were used to determine the sensible heat balance below the soil surface. Heat that cannot be accounted for directly by measurement, the residual to the soil sensible heat balance, is attributed to latent heat with evaporation of soil water. Comparisons of measured near-surface heat flux density with $LE + G$ in the traditional surface energy balance indicate that the soil heat flux is partitioned to LE below the surface, particularly several days after rainfall events. Combination of heat flux density measurements at multiple depths below the soil allows the location and magnitude of evaporation to be quantified, thereby revealing the dynamic evolution of soil water evaporation following rainfall events. Initial comparisons between daily estimates of heat balance evaporation compare favorably with standard independent methods for determining daily evaporation. However, unlike standard micrometeorological methods, large fetch is not a requirement. Because of its capability to measure evaporation with depth and time in field conditions, which is not available through other current approaches, the sensible heat balance method promises to be a practical and valuable addition for a wide range of vadose zone hydrology investigations.

[17] **Acknowledgments.** This work was supported by the National Science Foundation under Grant 0809656, by ConocoPhillips Company, and by Hatch Act, State of Iowa, and State of North Carolina funds.

References

Berge, H. F. M. (1990), *Heat and Water Transfer in Bare Topsoil and the Lower Atmosphere*, Cent. for Agric. Publ. and Doc., Wageningen, Netherlands.

Bland, W. L., J. T. Loew, and J. M. Norman (1996), Evaporation from cranberry, *Agric. For. Meteorol.*, *81*, 1–12, doi:10.1016/0168-1923(95)02304-6.

Bristow, K. L., G. J. Kluitenberg, and R. Horton (1994), Measurement of soil thermal properties with a dual-probe heat-pulse technique, *Soil Sci. Soc. Am. J.*, *58*, 1288–1294.

Cahill, A. T., and M. B. Parlange (1998), On water vapor transport in field soils, *Water Resour. Res.*, *34*, 731–739, doi:10.1029/97WR03756.

Campbell, G. S., C. Calissendorff, and J. H. Williams (1991), Probe for measuring soil specific heat using a heat-pulse method, *Soil Sci. Soc. Am. J.*, *55*, 291–293.

Cellier, P., G. Richard, and P. Robin (1996), Partition of sensible heat fluxes into soil and the atmosphere, *Agric. For. Meteorol.*, *82*, 245–265, doi:10.1016/0168-1923(95)02328-3.

Cobos, D. R., and J. M. Baker (2003), In situ measurement of soil heat flux with the gradient method, *Vados Zone J.*, *2*, 589–594.

Evett, S. R., A. W. Warrick, and A. D. Matthias (1995), Wall material and capping effects on microlysimeter temperatures and evaporation, *Soil Sci. Soc. Am. J.*, *59*, 329–336.

Fuchs, M. (1986), Heat flux, in *Methods of Soil Analysis, part 1, Physical and Mineralogical Methods*, *Soil Sci. Soc. of Am. Book Ser.*, vol. 5, 2nd ed., edited by A. Klute, pp. 957–968, Soil Sci. Soc. of Am., Madison, Wis.

Gardner, H. R., and R. J. Hanks (1966), Evaluation of the evaporation zone in soil by measurement of heat flux, *Soil Sci. Soc. Am. Proc.*, *30*, 425–428.

Ham, J. M., and E. J. Benson (2004), On the construction of dual-probe heat-capacity sensors, *Soil Sci. Soc. Am. J.*, *68*, 1185–1190.

Heilman, J. L., C. L. Brittin, and C. M. U. Neale (1989), Fetch requirements for Bowen ratio measurements of latent and sensible heat fluxes, *Agric. For. Meteorol.*, *44*, 261–273, doi:10.1016/0168-1923(89)90021-X.

Heitman, J. L., R. Horton, T. J. Sauer, and T. M. DeSutter (2008), Sensible heat observations reveal soil water evaporation dynamics, *J. Hydrometeorol.*, *9*, 165–171, doi:10.1175/2007JHM963.1.

Horton, R. (1989), Canopy shading effects on soil heat and water flow, *Soil Sci. Soc. Am. J.*, *53*, 669–679.

Jury, W. A., and B. Bellantuoni (1976), A background temperature correction for thermal conductivity probes, *Soil Sci. Soc. Am. J.*, *40*, 608–610.

Knight, J. H., and G. J. Kluitenberg (2004), Simplified computational approach for the dual-probe heat-pulse method, *Soil Sci. Soc. Am. J.*, *68*, 447–449.

Kondo, J., N. Saigusa, and T. Sato (1990), A parameterization of evaporation from bare soil surfaces, *J. Appl. Meteorol.*, *29*, 385–389, doi:10.1175/1520-0450(1990)029<0385:APOEFB>2.0.CO;2.

Lemon, E. R. (1956), The potentialities for decreasing soil moisture evaporation loss, *Soil Sci. Soc. Am. Proc.*, *20*, 120–125.

Mahrt, L., and H. Pan (1984), A two-layer model of soil hydrology, *Boundary Layer Meteorol.*, *29*, 1–20, doi:10.1007/BF00119116.

Mayocchi, C. L., and K. L. Bristow (1995), Soil surface heat flux: Some general questions and comments on measurements, *Agric. For. Meteorol.*, *75*, 43–50, doi:10.1016/0168-1923(94)02198-S.

Nassar, I. N., and R. Horton (1997), Heat, water, and solute transfer in unsaturated porous media: I. Theory development and transport coefficient evaluation, *Transp. Porous Media*, *27*, 17–38, doi:10.1023/A:1006583918576.

Ochsner, T. E., T. J. Sauer, and R. Horton (2006), Field tests of the soil heat flux plate method and some alternatives, *Agron. J.*, *98*, 1005–1014, doi:10.2134/agronj2005.0249.

Ochsner, T. E., T. J. Sauer, and R. Horton (2007), Soil heat capacity and heat storage measurements in energy balance studies, *Agron. J.*, *99*, 311–319.

Prat, M. (2007), On the influence of pore shape, contact angle, and film flows on drying of capillary porous media, *Int. J. Heat Mass Transfer*, *50*, 1455–1468, doi:10.1016/j.ijheatmasstransfer.2006.09.001.

Ren, T., T. E. Ochsner, and R. Horton (2003), Development of thermo-time domain reflectometry for vadose zone measurements, *Vadose Zone J.*, *2*, 544–551.

Sauer, T. J., and R. Horton (2005), Soil heat flux, in *Micrometeorology in Agricultural Systems*, *Agron. Monogr.*, vol. 47, edited by J. L. Hatfield and J. M. Baker, pp. 131–154, Am. Soc. of Agron., Madison, Wis.

Sauer, T. J., P. A. Moore Jr., J. M. Ham, W. L. Bland, J. H. Prueger, and C. P. West (2002), Seasonal water balance of an Ozark hillslope, *Agric. Water Manage.*, *55*, 71–82, doi:10.1016/S0378-3774(01)00185-8.

Segura, L. A., and P. G. Toledo (2005), Pore-level modeling of isothermal drying of pore networks: Effects of gravity and pore shape and size distributions on saturation and transport parameters, *Chem. Eng. J.*, *111*, 237–252, doi:10.1016/j.cej.2005.02.004.

Wetzel, P. J., and J. T. Chang (1987), Concerning the relationship between evapotranspiration and soil moisture, *J. Clim. Appl. Meteorol.*, *26*, 18–27, doi:10.1175/1520-0450(1987)026<0018:CTRBEA>2.0.CO;2.

Yamanaka, T., and T. Yonetani (1999), Dynamics of the evaporation zone in dry sandy soils, *J. Hydrol.*, *217*, 135–148, doi:10.1016/S0022-1694(99)00021-9.

Yamanaka, T., A. Takeda, and J. Shimada (1998), Evaporation beneath the soil surface: Some observational evidence and numerical experiments, *Hydrol. Processes*, *12*, 2193–2203, doi:10.1002/(SICI)1099-1085(19981030)12:13/14<2193::AID-HYP729>3.0.CO;2-P.

J. L. Heitman, Department of Soil Science, North Carolina State University, Campus Box 7619, Raleigh, NC 27695, USA. (jlheitman@ncsu.edu)

R. Horton and X. Xiao, Department of Agronomy, Iowa State University, 2101 Agronomy Hall, Ames, IA 50011, USA.

T. J. Sauer, National Soil Tilth Laboratory, Agricultural Research Service, United States Department of Agriculture, 2110 University Boulevard, Ames, IA 50011, USA.